Journal of the Serbian Chemical Society
JSCS-info@shd.org.rs • www.shd.org.rs/JSCS

J. Serb. Chem. Soc. *78* (12) 2115–2130 (2013)
JSCS–4554

UDC 546.131+544.6.076.32–13:66.094.3:
541.135:544.4
Original scientific paper

The kinetics of hydrogen chloride oxidation•

ISAI GONZALEZ MARTINEZ[1], TANJA VIDAKOVIĆ-KOCH[2]*, RAFAEL KUWERTZ[3], ULRICH KUNZ[3], THOMAS TUREK[3] and KAI SUNDMACHER[1,2]

[1]Otto-von-Guericke University, Process Systems Engineering, Universitätsplatz 2, 39106 Magdeburg, Germany, [2]Max-Planck Institute for Dynamics of Complex Technical Systems, Sandtorstrasse 1, 39106 Magdeburg, Germany, and [3]Institute of Chemical Process Engineering, Clausthal University of Technology, Leibnizstr. 17, 38678 Clausthal-Zellerfeld, Germany

(Received 19 November 2013)

Abstract: Hydrogen chloride (HCl) oxidation was investigated on technical membrane electrode assemblies in a cyclone flow cell. The influences of Nafion loading, temperature and hydrogen chloride mole fraction in the gas phase were studied. The apparent kinetic parameters, such as reaction order with respect to HCl, Tafel slope and activation energy, were determined from the polarization data. The apparent kinetic parameters suggest that the recombination of adsorbed Cl intermediate is the rate-determining step.

Keywords: gas diffusion electrodes, Nafion, electrolysis, HCl gas phase oxidation, kinetics.

INTRODUCTION

Anhydrous gaseous HCl is a by-product of different reactions in the plastics industry, for example during production of isocyanates by treating amines with phosgene.[1] This by-product is commonly absorbed in water or neutralized. A further option for handling gaseous HCl is its recycling back to chlorine. This option is more advantageous since chlorine is a high value product with a number of applications in the chemical industry. HCl can be chemically or electrochemically converted to chlorine.[2] The chemical process follows the so-called Deacon stoichiometry: $4HCl + O_2 \rightarrow 2Cl_2 + 2H_2O$.

This process was initially outperformed by electrochemical processes, but, due to the recent advances in ruthenium-based catalysts, it has been successfully revisited.[3] Still, even with the present progress in heterogeneous chemical catal-

* Corresponding author. E-mail: vidakovic@mpi-magdeburg.mpg.de
• Dedicated to the 70th birthday of Prof. Branislav Nikolić.
doi: 10.2298/JSC131119142G

ysis, electrochemical processes outperform chemical HCl oxidation in terms of the investment costs per ton of chlorine, the possibility of module-based (decentralized) operation[4] and the required process temperature (*ca*. 343 K in the electrochemical compared to 453–773 K for the chemical process[3]). The major electrochemical routes for recycling chlorine back from HCl were summarized in recent publications.[4–6] To recapitulate shortly, the state-of-the-art electrochemical process (DuPont–DeNora) is based on direct splitting of HCl into chlorine and hydrogen: $2HCl \rightarrow Cl_2 + H_2$

Further developments in the electrochemical recycling of HCl were mainly directed towards an increase in energy efficiency. In this respect, the major savings were obtained by influencing the thermodynamics of the process through change in the aggregate state of the reactant or by changing the process stoichiometry. The change in the process stoichiometry by introducing an oxygen-consuming instead of a hydrogen-evolving cathode resulted in *ca*. 30 % energy saving compared to the state-of-the-art process.[6] This so-called Bayer–Hoechst–Uhde process with an overall process stoichiometry corresponding to the Deacon process has already been realized on the technical scale. Aqueous HCl is employed in this process. It was demonstrated recently that utilization of gaseous instead of aqueous HCl resulted in an additional energy saving (up to 50 % compared to that obtained in the state-of-the-art process).[5]

Further development and optimization of this promising process variant requires detailed knowledge of the reaction kinetics. In this respect, especially kinetic information on the electro-oxidation of gaseous HCl are extremely rare.[7] To obtain meaningful information for process development, kinetic measurements have to be performed under technically realistic conditions using membrane electrode assemblies (MEA), and keeping simultaneously the influence of the counter electrode and the membrane negligible. These conditions can be realized in a specially designed electrochemical cell, the so-called cyclone flow cell. The advantages of this special experimental set-up have been exemplified in previous publications.[8–10] Recently, this set-up was employed for an investigation of the influence of structural parameters of MEA on HCl oxidation.[6] The determination of apparent kinetic parameters, such as Tafel slopes, reaction order with respect to HCl and the activation energy for HCl oxidation are the focus of this contribution. The kinetic parameters were determined between room temperature and 60 °C and for MEAs comprising different Nafion loadings. The significance of these apparent parameters was further evaluated with respect to possible mechanisms of HCl oxidation.

EXPERIMENTAL

Membrane electrode assembly (MEA) preparation

The MEA was composed of a gas diffusion layer (GDL) and a catalyst layer (CL) sprayed over a Nafion 117 membrane by a wet-spraying method as described in the lierature.[5] 60 mass

% platinum supported on Vulcan XC72R (BASF) was employed as the catalyst. The catalyst-sprayed membrane was hot-pressed for 3 min at 90 kg cm^{-2}. The total geometrical active MEA area was 2 cm^2.

Electrochemical measurements

All measurements were performed in a cyclone flow cell as described in the literature.[6] Hydrogen chloride was diluted with nitrogen in order to attain the desired concentrations. The cell was kept in a convection oven with integrated temperature control (Mammert UNP500) in order to maintain the system at the desired reaction temperature.

The electrodes were pre-conditioned by cyclic voltammetry in the range from 0.2 to 1.0 V *vs*. Ag/AgCl with a sweep rate of 50 mV s^{-1} for 10 cycles. Polarization curves were obtained under quasi-steady state conditions using linear sweep voltammetry with a Solarton 1286 potentiostat at a sweep rate of 1 mV s^{-1}. Ohmic drop compensation was employed *via* the current interrupt method. Before each temperature change, a linear sweep with N_2 was recorded and employed as a base line correction for all measurements with hydrogen chloride. The baseline corrections never exceeded 7 % of the total current. The results presented in this work are the average of at least three measurements. All potentials are expressed vs. standard hydrogen electrode (SHE).

RESULTS

Origin of limiting current behavior

Polarization curves for the electro-oxidation of gaseous HCl at MEAs comprising different Nafion loadings at constant platinum loading (0.5 mg cm^{-2}) are shown in Fig. 1. As can be seen, all electrodes reach technical current densities (300 to 400 mA cm^{-2}) at relatively low overpotentials. The optimization of the Nafion loading resulted in an increase in catalyst utilization. In addition, the increase in Nafion loading decreases the reaction overpotential (*ca*. 40 mV for the electrodes comprising the highest with respect to lowest Nafion loading at 400 mA cm^{-2}). Although the difference is not strikingly high, it still has importance for energy saving in this process, especially taking into account that technical electrolysis systems operate at high current densities.

The maximal current densities observed in the present study were similar to those reported by Eames and Newman[7] in a solid-polymer electrolyte reactor for electrochemical conversion of anhydrous HCl to Cl_2. However, the overpotentials (expressed relative to the open circuit potentials) of *ca*. 200 mV in the present study are much lower compared to those obtained in the study of Eames and Newman[7] study (*ca*. 1 V). This significant difference might be partly due to an improved MEA structure in the present case. In addition, the data of Eames and Newman[7] accounts not only for the voltage losses related to the anode (as here), but incorporate also the losses on the cathode side and in the membrane. The membrane losses can be significantly high, since the conductivity of Nafion strongly decreases in the presence of HCl.[14]

As can be seen in Fig. 1, all studied the MEAs showed limiting current behavior at more positive overpotentials. The limiting currents were also observed

in the study with gaseous HCl oxidation[7] as well as in studies where chlorine evolution from aqueous HCl[11] or NaCl[12] were investigated. In the study with gaseous HCl,[7] as possible sources of limiting behavior, the limitations caused by the membrane and gas-phase mass transfer were discussed, and it was concluded that the main cause for the experimentally observed limiting behavior was low membrane conductivity due to dehydration. In the study on chlorine evolution from brine solution, Conway and Ping[12] considered limitations by slow diffusion of the product chlorine. They performed their experiments using a rotating disc electrode and observed only a small effect of the electrode rotation on the reaction rate, which led them to the conclusion that the chemical step, *i.e.*, chlorine recombination, and not diffusion effects limited the currents at more positive overpotentials.

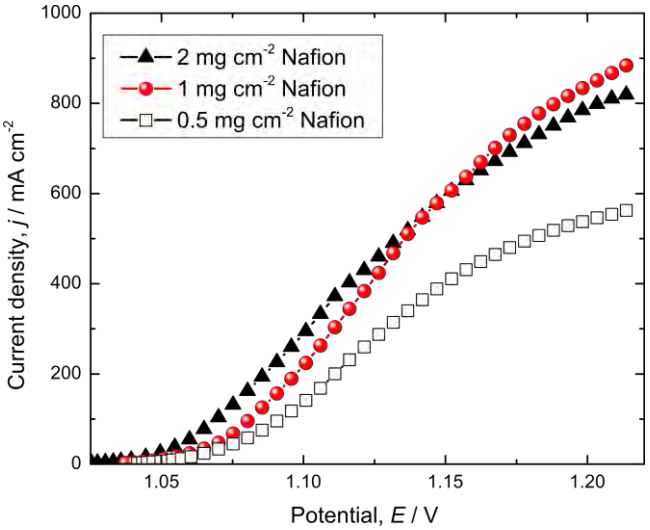

Fig. 1. Influence of Nafion loading at constant platinum loading (0.5 mg cm^{-2}) on HCl oxidation. Conditions: temperature: 60 °C, pressure: 101.3 kPa, HCl flow rate: 500 ml min^{-1} and sweep rate: 1 mV s^{-1}.

In the present study, since the MEA consists of several layers of different thicknesses and porosities, different mass transfer resistances or combinations of them can contribute to the observed limiting behavior. In addition, electrochemical reaction itself can be limiting. To estimate the effects of single resistances, analysis with dimensionless numbers, as is common in chemical reaction engineering and as shown by Vidaković *et al.*[9] using as an example methanol electrooxidation, was employed. Two kinds of dimensionless numbers were considered, the Biot number for the estimation of diffusion resistances in the adherent layers where only the diffusion occurs and the so-called second Damköhler number that is used in reacting systems with diffusion. The second Damköhler number is

defined as the ratio of the resistance of diffusion and resistance of electrochemical reaction as follows:

$$Da_{\mathrm{II}} = \frac{\delta_{\mathrm{CL}}\, j}{nFc_{\mathrm{HCl}} D_{\mathrm{HCl}}^{\mathrm{CL}}} \tag{1}$$

where δ_{CL} is the thickness of the catalyst layer (*ca*. 20 μm), j is the current density (*ca*. 9 kA m^{-2}), c_{HCl} the HCl gas phase concentration (36.6 mol m^{-3} assuming ideal gas behavior at 101.3 kPa and 60 °C) and $D_{\mathrm{HCl}}^{\mathrm{CL}}$ the HCl diffusion coefficient in the CL (2.10×10^{-6} m^2 s^{-1}). The HCl diffusion coefficient in the CL accounts for the porosity of the layer (*ca*. 20 %); furthermore, it has been assumed that the void fraction in the CL is filled with the gas phase. The given data result in a Damköhler number of $Da_{\mathrm{II}} \approx 0.012$. This value indicates that the resistance of the electrochemical reaction is bigger than the resistance of the diffusion.

The relevance of the mass transport resistance in the gas diffusion layer (GDL) was estimated by means of the following Biot number (*Bi*):

$$Bi^{\mathrm{GDL/CL}} = \frac{D_{\mathrm{HCl}}^{\mathrm{CL}} / \delta_{\mathrm{CL}}}{D_{\mathrm{HCl}}^{\mathrm{GDL}} / \delta_{\mathrm{GDL}}} \tag{2}$$

where $D_{\mathrm{HCl}}^{\mathrm{GDL}}$ is the effective HCl diffusion coefficient in the GDL (8.63×10^{-6} m^2 s^{-1}) and δ_{GDL} is the thickness of the GDL (*ca*. 250 μm). The calculated value of this Biot number is *ca*. 3, which means that the mass transfer resistance in the GDL is 3 times higher than in the CL. This reflects the fact that the GDL is *ca*. 12 times thicker than the CL (250 *vs*. 20 μm), while the diffusion coefficient in the GDL is only *ca*. 4 times greater than in the CL (8.63×10^{-6} *vs*. 2.10×10^{-6} m^2 s^{-1}).

The relevance of the external film resistance in relation to the resistance of diffusion exerted by the GDL can be estimated in a similar manner:

$$Bi^{\mathrm{HDL/GDL}} = \frac{D_{\mathrm{HCl}}^{\mathrm{GDL}} / \delta_{\mathrm{GDL}}}{k_{\mathrm{m}}} \tag{3}$$

where k_{m} is the film mass transfer coefficient (1.61×10^{-3} m s^{-1}, calculated based on correlation provided by Schultz and Sundmacher[13]). The calculated value of $Bi^{\mathrm{HDL/GDL}}$ based on the given data is *ca*. 20.

Multiplying Da_{II} with the Biot numbers defined above yields the electrochemical reaction rate (resistance of electrochemical reaction) in relation to the mass transfer rates, i.e., resistance of diffusion in GDL and resistance of external film diffusion, respectively:

$$Da_{\mathrm{II}} Bi^{\mathrm{GDL/CL}} \approx 0.036 \tag{4}$$

$$Da_{\mathrm{II}} Bi^{\mathrm{GDL/CL}} Bi^{\mathrm{HDL/GDL}} \approx 0.72 \tag{5}$$

The last expression gives the ratio between all mass transfer resistances and the resistance of electrochemical reaction and shows that the two resistances are comparable.

Determination of the apparent kinetic parameters

Tafel slope values. For complex electrochemical reactions involving diffusion, electrochemical and chemical steps, it can be shown that in the steady state:[14]

$$\frac{1}{j_{\text{meas}}} = \frac{1}{j_{\text{diff}}} + \frac{1}{j_{\text{react}}} + \frac{1}{j_{\text{kin}}} \tag{6}$$

where on the right hand side only the last term will be dependent on the potential. This equation demonstrates that at more positive overpotentials, the reaction rate can become limited by diffusion (j_{diff}) or chemical reaction (j_{react}). Since the previous analysis showed that, under the present conditions and at more positive overpotentials, the current is probably diffusion–reaction-limited, one can use the Eq. (6) for an estimation of the rate of the electrochemical step (j_{kin}) in accordance to:

$$j_{\text{kin}} = \frac{j_{(\text{diff,react})} j_{\text{meas}}}{j_{(\text{diff,react})} - j_{\text{meas}}} \tag{7}$$

where the values of $j_{(\text{diff,react})}$ can be estimated from the experimental data (Fig. 1) at more positive overpotentials. The calculated values of j_{kin} can be now plotted against the electrode potential in the form of a Tafel plot (Fig. 2). As can be seen in Fig. 2, irrespective of the Nafion loading, two linear regions could be observed with a lower Tafel slope value of *ca*. 30 mV dec^{-1} at low overpotentials, followed by a higher Tafel slope value of *ca*. 60 mV dec^{-1} at high overpotentials.

In a similar way, the experimental data for MEA comprising 0.5 mg cm^{-2} platinum and 1 mg cm^{-2} Nafion at a constant temperature of 60 °C and at varying partial pressures of HCl in the gas phase was analyzed, as shown in Fig. 3. Again, two linear regions are clearly seen but only in the experiments at higher HCl partial pressures, while at lower partial pressures, these two regions merge into one with an effective Tafel slope of *ca*. 40–45 mV dec^{-1}.

The MEA of the same composition was further tested at varying temperatures with the other conditions being kept constant. The results presented in Fig. 4 show two distinct linear regions in the temperature range from 40–60 °C. The Tafel slope values in these two regions were virtually independent of temperature. At room temperature, the transition from low Tafel slope region to high Tafel slope region was more gradual with an intermediate Tafel slope value of *ca*. 40 mV dec^{-1}.

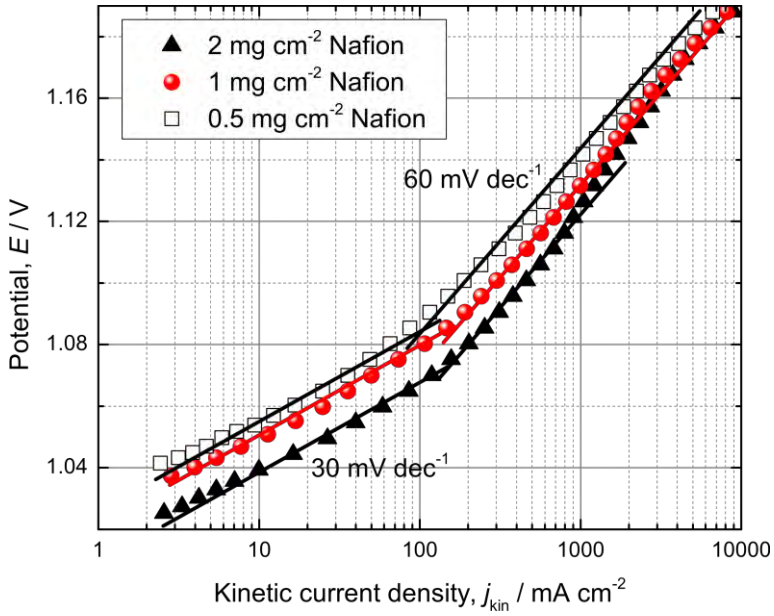

Fig. 2. Tafel plot for the HCl oxidation on an MEA comprising a constant Pt loading (0.5 mg cm^{-2}) and different Nafion loadings. Conditions as in Fig. 1.

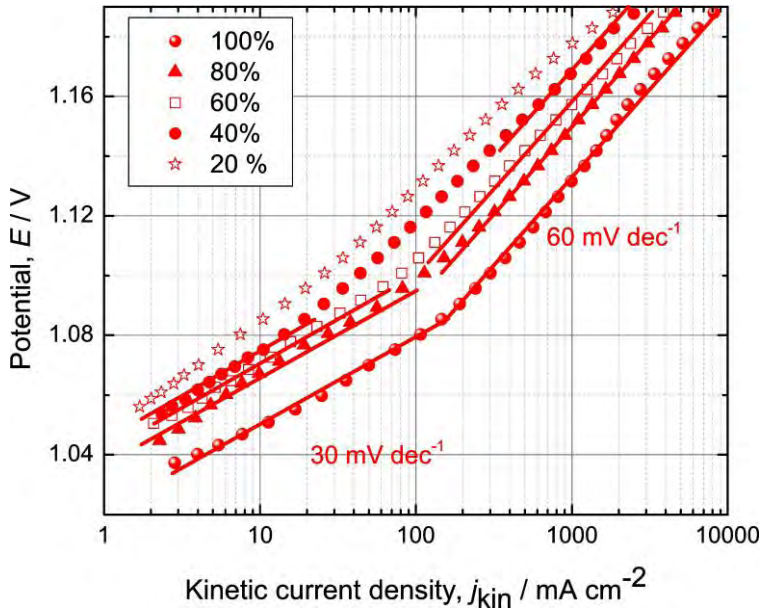

Fig. 3. Influence of HCl partial pressure on HCl oxidation on an MEA comprising 0.5 mg cm^{-2} Pt and 1 mg cm^{-2} Nafion. Conditions: temperature: 60 °C, pressure: 101.3 kPa, HCl flow rate: 500 ml min^{-1} and sweep rate: 1 mV s^{-1}.

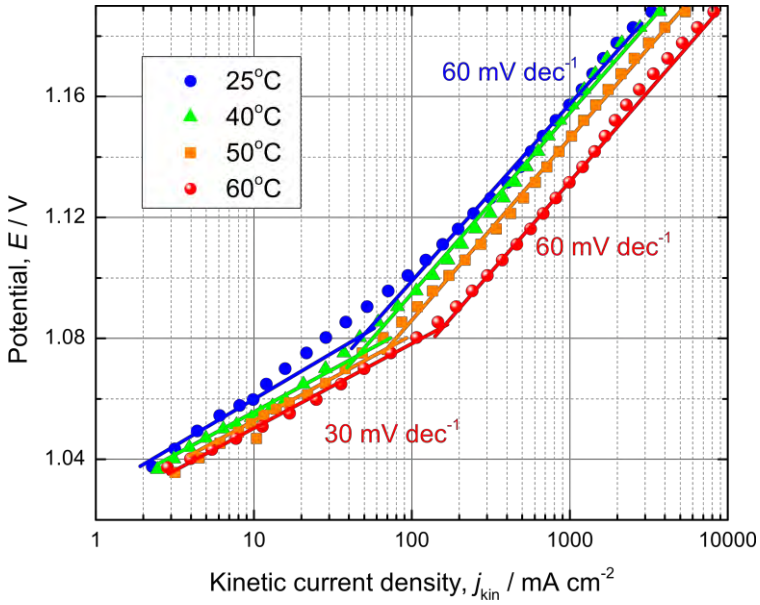

Fig. 4. Influence of temperature on HCl oxidation on an MEA comprising 0.5 mg cm^{-2} Pt and 1 mg cm^{-2} Nafion. Conditions: HCl pressure: 101.3 kPa, HCl flow rate: 500 ml min^{-1} and sweep rate: 1 mV s^{-1}.

Apparent reaction order. In addition to the Tafel slope, the reaction order is an important kinetic parameter for discrimination between different reaction mechanisms. In the present study, the apparent reaction orders were calculated from the slope of ln j_{kin} *vs.* ln y_{HCl} plot at constant electrode potentials (Fig. 5). The calculated values were 0.82±0.07, 1.07±0.09 and 0.97±0.07 at 1.065, 1.095 and 1.155 V, respectively. For the calculations, only the points up to 0.8 mole fraction HCl were considered. As can be seen in Fig. 5, the last points corresponding to pure HCl gas lay out of the trend lines at all potentials.

The apparent activation energies. The apparent activation energies were calculated from Arrhenius plots at constant overpotentials (Fig. 6a). The obtained values changed from *ca*. 16 kJ mol^{-1} at low overpotentials to *ca*. 30 kJ mol^{-1} at intermediate values of the overpotentials. At very positive overpotentials, again values around 16 kJ mol^{-1} were obtained (Fig. 6b).

DISCUSSION

The onset vs. *equilibrium electrode potential, gas or liquid phase HCl oxidation*

In the present experiments, HCl was introduced as a reactant in the gas phase. However, in the employed experimental set-up, the Nafion membrane was from one side equilibrated with acid and therefore fully humidified. Water from the Nafion membrane could also enter the CL, which under some conditions can

lead to flooding of the void fraction of the CL. In this scenario, HCl from the gas phase absorbs in water prior to electrochemical reaction according to:

$$\mathrm{HCl(g)} \rightarrow \mathrm{HCl(aq)} \tag{8}$$

$$\mathrm{HCl(aq)} \rightarrow \mathrm{H^+(aq) + Cl^-(aq)} \tag{9}$$

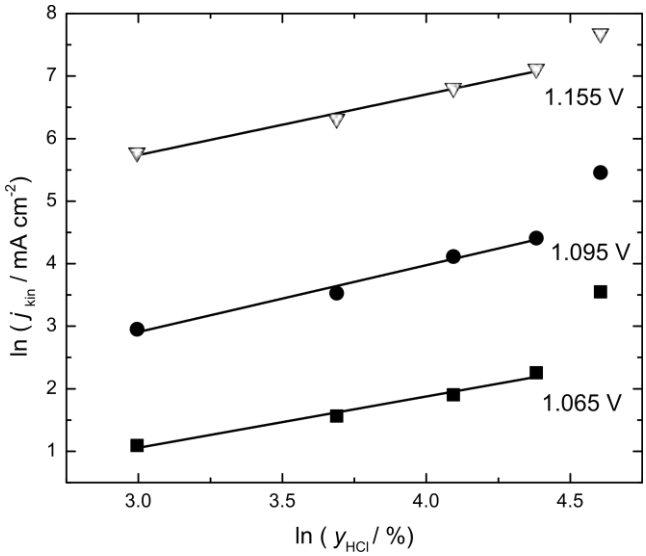

Fig. 5. Apparent reaction order with respect to the HCl concentration expressed in terms of HCl mole fraction (in %) in the gas phase. Data extracted from Fig. 3.

The chlorine ion reacts further electrochemically according to the well-known reaction for chlorine evolution from, *e.g.*, brine solution:

$$\mathrm{2Cl^-(aq) \rightarrow Cl_2(g) + 2e^-} \tag{10}$$

If reactions (8) and (9) are multiplied with 2 and summed with reaction (10), one obtains:

$$\mathrm{2HCl(g) \rightarrow Cl_2(g) + 2H^+(aq) + 2e^-} \tag{11}$$

this corresponds to the case of direct HCl oxidation from the gas phase.

The standard equilibrium potentials of reactions (10) and (11) are significantly different with values of 1.358 and 0.988 V, respectively. The observed open circuit potentials in the present work were around 1.03 V. This value is closer to the standard equilibrium potential of the gas phase reaction (Eq. (11)). Under the present conditions, a deviation from the standard value could be caused by deviations in the proton activity and the chlorine partial pressure from their standard values. The temperature dependence with a temperature coefficient of –0.1 mV K^{-1} (calculated based on literature data[15]) is not strongly expressed (which

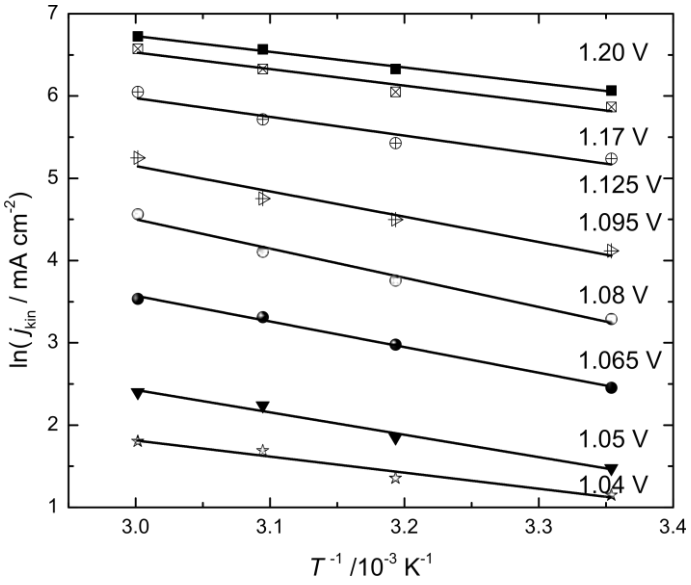

(a)

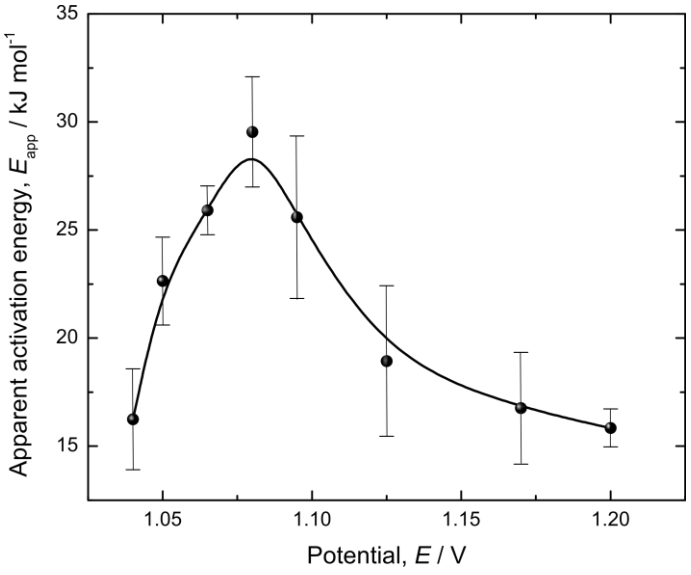

(b)

Fig. 6. a) Arrhenius plots for HCl oxidation on an MEA comprising 0.5 mg cm^{-2} Pt and 1 mg cm^{-2} Nafion (data extracted from Fig. 4) and b) dependence of the apparent activation energies on potential.

also corresponds to the experimental observations in Fig. 4). The proton activity is given by the activity of protons in the Nafion membrane, which at 60 °C is *ca*.

2.[16] This deviation from the standard conditions contributes to a *ca*. 16 mV increase in the equilibrium potential, which would result in a value close to the experimentally observed one. However, it should be mentioned that the chlorine activity was not controlled under the employed conditions, and this effect would decrease the equilibrium potential value.

The standard potential of the liquid phase reaction (Eq. (10)) is much more positive than the observed experimental values. However, assuming the formation of a very concentrated HCl solution (*e.g*., 30 mass %) and taking into account the high non-ideality of such a solution, a reduction of the standard value by *ca*. –140 mV could be obtained. The deviation of the chlorine activity from standard conditions would cause a further lowering compared to the value under standard conditions, which could bring this potential eventually close to the measured values. The temperature dependence for this reaction with a temperature coefficient of *ca*. –1.2 mV K^{-1} is more pronounced than for the reaction (Eq. (11)) resulting in a *ca*. –40 mV difference between the values at room temperature and 60 °C.

The experimentally observed deviation with temperature (Fig. 4) was only *ca*. –3 mV, which could be an argument for the gas phase reaction (Eq. (11)). However, the less explicit dependence of measured open circuit potentials than expected for the liquid phase reaction could be the consequence of the temperature influence on the gas–liquid equilibrium (reactions (8) and (9)). Consequently, the expected molality of chlorine ions in the liquid phase at room temperature would be higher (*ca*. 15.5 mol kg^{-1}) than at 60 °C (*ca*. 12 mol kg^{-1}). Taking into account that the HCl acid deviation from ideality at room temperature was more expressed than at elevated temperatures (molal activity coefficients 37.55 and 9.83 at room temperature and 60 °C, respectively[17]) a value of *ca*. 26 mV could be calculated based on this effect. In addition, the membrane potential would contribute in a similar manner, giving a virtually unchanged potential value, as was observed in the experiments.

In the experiments with varying partial pressures of hydrogen chloride at 60 °C, the experimentally observed difference of the open circuit potentials between the lowest and highest HCl partial pressures was *ca*. 19 mV. Assuming ideal gas behavior for HCl under all conditions, a deviation of *ca*. 46 mV could be expected. If a reaction from the liquid phase is assumed, a deviation of *ca*. 55 mV could be obtained. Both values are significantly different compared to the experimentally observed value.

The measured open circuit potential values are additionally influenced by junction potentials in the present experimental set-up. The most significant one is the membrane potential, the so-called Donnan potential.[15] The Donnan potential is caused by the different activities of protons inside the membrane and in interfacing solutions. In the case of the liquid phase reaction (Eq. (10)), assuming the

activity of protons is the same as that of chlorine ions; a value of *ca*. –140 mV (calculated for 60 °C) could be obtained. This value will be different in the case of the gas phase reaction (Eq. 11), since in this case, the Donnan potential is formed only at the liquid/membrane interface, giving a value of *ca*. –20 mV (calculated for 60 °C). It should also be mentioned that in the experiments with varying temperature or partial pressure of HCl, the Donnan potential would be also influenced through changes in the proton activities.

Finally, the measured values are influenced by the diffusion potential at the interface of the reference electrode and the liquid acid, which is difficult to calculate for the case of concentrated solutions. An estimation based on the Henderson Equation[15] gives a value of *ca*. 3 mV, which is significantly smaller than the Donnan potential.

To summarize, the presence of junction potentials and the uncertainty in the effect of the partial pressure of chlorine on the equilibrium conditions of the reactions (Eqs. (10) and (11)), makes it difficult to conclude which of these two reactions effectively determines the observed open circuit values.

Mechanism of HCl oxidation

The only proposed mechanism for the gaseous HCl oxidation (corresponding to overall reaction Eq. (11)) was presented by Eames and Newman,[7] Eqs. (A-1) and (A-2), with the chemical reaction (A-2) as a rate determining step (r.d.s.). This mechanism will be further denoted as mechanism "A":

$$\mathrm{HCl(g)} + \mathrm{Pt} \square \quad \mathrm{PtCl} + \mathrm{H^+(aq)} + \mathrm{e^-} \qquad \text{(A-1)}$$

$$2\mathrm{PtCl} \rightarrow 2\mathrm{Pt} + \mathrm{Cl_2(g)} \qquad \text{(A-2)}$$

It is also possible to assume that both steps proceed as electrochemical reactions:

$$\mathrm{HCl(g)} + \mathrm{Pt} \square \quad \mathrm{PtCl} + \mathrm{H^+(aq)} + \mathrm{e^-} \qquad \text{(B-1)}$$

$$\mathrm{HCl(g)} + \mathrm{PtCl} \rightarrow \mathrm{Pt} + \mathrm{Cl_2} + \mathrm{H^+(aq)} + \mathrm{e^-} \qquad \text{(B-2)}$$

This mechanism will be further denoted as mechanism "B".

Alternatively, if instead of the overall reaction (Eq. (11)), the overall reaction (Eq. (10)) would be valid, similar reaction mechanisms could be formulated, simply by replacing HCl(g) with Cl^-(aq). Additionally, protons would disappear from the expressions for mechanisms "A" and "B". The presence of protons appears to be an important criterion to differentiate between the overall reactions Eqs. (10) and (11), since for reaction Eq. (10), the protons should not have any influence on the equilibrium conditions. However, Boggio *et al.*[18] determined a reaction order with respect to protons of –1 in the case of chlorine evolution from brine. This could indicate that in addition to previously mentioned chlorine species, also non-dissociated HCl(aq), reaction Eq. (9), could be a potential source

of chlorine. Presently, as was previously discussed, it is not possible to assign which overall reaction occurs, but the following analysis is not affected by this uncertainty.

The mechanisms "A" and "B" with Cl^- as the reacting species were previously introduced by Gileadi.[19] He assumed that in both mechanisms, the second reaction was the rate determining one, which was further assumed to be irreversible. The first step was always assumed to be in quasi-equilibrium. In his analysis, the pre-exponential term in the Frumkin isotherm, assuming effectively the so-called Temkin isotherm, was neglected. With these assumptions, the values of Tafel slopes and the reaction orders for different degrees of coverage at the electrode surface were determined. The data that have been recalculated for the temperature range in the present study are presented in Table I.

TABLE I. Tafel slopes and reaction orders with respect to HCl calculated based on literature data[19]

Coverage	Mechanism "A"		Mechanism "B"	
	Tafel slope mV dec^{-1}	Reaction order	Tafel slope mV dec^{-1}	Reaction order
Low ($\theta \to 0$)	17–19	2	13–14	2
Intermediate ($0.2 < \theta < 0.8$)	26–29	1.5	26–29	1
High ($\theta \to 1$)	51–57	1	∞	–

The Tafel slope values that were observed in the present study are in the range from *ca*. 30 mV dec^{-1} at low overpotentials to *ca*. 60 mV dec^{-1} at high overpotentials. These values were relatively temperature independent. The only exception was the value at room temperature with a slope of *ca*. 40 mV dec^{-1}) at low overpotentials. In the experiments with changing HCl partial pressure, the Tafel slope values also changed from 30 to 60 mV dec^{-1} for low and high overpotentials. These values were concentration dependent with an average Tafel slope of *ca*. 40–45 mV dec^{-1} at low HCl partial pressure. If these values are compared with the theoretical predictions in Table I, good agreement between the calculated values for mechanism "A", with a chemical step as a rate determining step, at intermediate and high degrees of coverage with adsorbed intermediates, and the experimental one could be registered. Mechanism "B" can obviously be disregarded, since at high coverage, it predicts an infinite Tafel slope value. Slightly different Tafel slope values under low temperature conditions and low HCl partial pressures could obviously be the consequence of the influence of temperature and concentration on the degree of coverage with adsorbed intermediates.[6]

The second apparent kinetic parameter that was determined in the present paper was the reaction order with respect to HCl. The determined values were *ca*. 0.82, 1.07 and 0.97 for 1.065, 1.095 and 1.155 V, respectively. The first two

values correspond to the region of the first Tafel slope (intermediate coverage of adsorbed intermediate) and the last value to the region of the second Tafel slope (high coverage of adsorbed intermediate). The theoretical values in Table I are between 1.5 and 1 for mechanism "A". As can seen, the apparent values deviate from calculated ones, which was especially evident in the first Tafel slope region. It should be recalled here that the last points in Fig. 5 corresponding to pure HCl were off trend lines at all potentials. Inclusion of these points obviously resulted in an increase in the apparent reaction orders, but straight lines in that case would have very low linear coefficients, making them unreliable. Since the gas–liquid equilibrium of the HCl(g) – water system exhibited high non-linearities (especially in the range of low and high HCl partial pressures) and taking into account the previous discussion on gas or liquid phase HCl oxidation, the data in Fig. 5 was recalculated with respect to Cl^- activities. It was assumed that the Cl^- activity coefficient was the same as the mean activity coefficient of the acid. The recalculated data are presented in Fig. 7. As can be seen, the data at all potentials in the whole range of studied activities followed the trend lines. The slopes of these trend lines were 1.27±0.06, 1.29±0.07 and 0.98±0.12 for 1.065, 1.095 and 1.155 V, respectively. The new calculated values are in much better agreement with the theoretical values in Table I for the case of mechanism "A" with the chemical step (recombination of adsorbed Pt–Cl) as the rate-determining step.

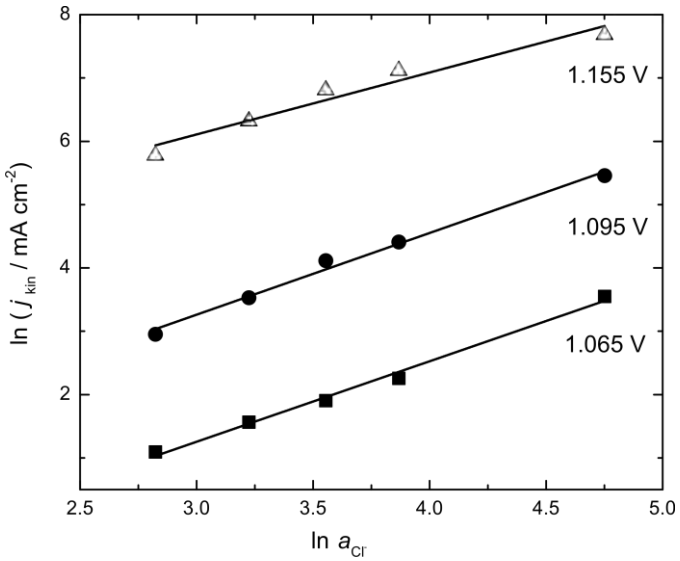

Fig. 7. Apparent reaction order with respect to HCl concentration expressed in terms of Cl^- activity in the liquid phase. Kinetic current densities are extracted from Fig. 3.

Finally, the determined values of the apparent activation energies in the range from 16 to 30 kJ mol^{-1} support further Pt–Cl recombination (Eq. (A-2)) as

the rate determining step.[19] As can be seen in Fig. 6b, the apparent activation energy is potential dependent. This was expected since the apparent values include also the contribution of the electrochemical activation. Additionally, the observed trend indicates the dependence of the activation energies on the surface coverage with Pt–Cl. The increase in the apparent activation energies at more negative overpotentials (first Tafel slope region) was probably caused by an increase of the Pt–Cl surface coverage. At more positive potentials, the overall values decrease due to the higher dominance of electrochemical activation as well as smaller changes in the apparent activation energies because of the very high Pt–Cl coverage.

CONCLUSIONS

The kinetics of HCl oxidation was studied on technical MEAs comprising different Nafion loadings at constant Pt loading. The influence of temperature and HCl partial pressure was studied for a selected MEA comprising 0.5 mg cm^{-2} Pt and 1 mg cm^{-2} Nafion. It was found that the HCl oxidation at industrially relevant current densities was viable on all studied MEAs. The optimization of the Nafion loading resulted in an increase of the catalyst utilization and a reduction in the reaction overpotential. An analysis with dimensionless numbers showed that the current at more negative overpotentials was at mixed reaction–diffusion-limitations.

Analysis of the apparent reaction order and Tafel slopes showed that the most viable mechanism to describe gaseous HCl oxidation is the one assuming dissociative electrochemical adsorption of reacting chlorine species and chemical recombination of the adsorbed Pt–Cl as the rate-determining step. According to this mechanism, the reaction proceeded under conditions of intermediate and high degree of coverage with adsorbed Pt–Cl.

A significant question in the present analysis was the question of whether a gas or liquid HCl oxidation mechanism applies. It was shown that based on the values of the open circuit potentials and their dependences on the operating parameters (temperature and HCl partial pressure), it is not possible to distinguish between these two scenarios. As was discussed, the appearance of different junction potentials in the system, where the membrane potential is probably the most influencing one, makes this analysis even more difficult. However, the dependence of the kinetic currents on the Cl^- activity adds some argument for liquid HCl oxidation.

Acknowledgments. The authors are grateful to the German Research Foundation (Deutsche Forschungsgemeinschaft, DFG) for financial support of this research work under the Project Grants SU 189/4-1 and KU 853/5-1. TVK is grateful to Prof. Mihai Christov (University of Chemical Technology and Metallurgy, Department of Physical Chemistry, 1756 Sofia, Bulgaria) for fruitful discussion on electrode kinetics.

ИЗВОД

КИНЕТИКА ОКСИДАЦИЈЕ ХЛОРОВОДОНИКА

ISAI GONZALEZ MARTINEZ[1], TANJA VIDAKOVIĆ-KOCH[2], RAFAEL KUWERTZ[3], ULRICH KUNZ[3], THOMAS TUREK[3] и KAI SUNDMACHER[1,2]

[1]Otto-von-Guericke University, Process Systems Engineering, Universitätsplatz 2, 39106 Magdeburg, Germany, [2]Max-Planck Institute for Dynamics of Complex Technical Systems, Sandtorstrasse 1, 39106 Magdeburg, Germany и [3]Institute of Chemical Process Engineering, Clausthal University of Technology, Leibnizstr. 17, 38678 Clausthal-Zellerfeld, Germany

Оксидација хлороводоника је проучавана на техничким гасно-дифузионим електродама у циклонској ћелији. Испитиван је утицај количине нафиона у каталитичком слоју, температуре и молског удела хлороводоника у гасовитој фази на кинетику ове реакције. На основу мерења одређени су привидни кинетички параметри, као што су ред реакције по хлороводонику, Тафелов нагиб и енергија активације. Вредности ових параметара указују на то да је рекомбинација адсорбованих атома хлора спори ступањ у реакцији.

(Примљено 19. новембра 2013)

REFERENCES

1. C. Six, F. Richter, in *Ullmann's Encyclopedia of Industrial Chemistry*, Wiley-VCH, 2000
2. P. Schmittinger, T. Florkiewicz, L. C. Curlin, B. Lüke, R. Scannell, T. Navin, E. Zelfel, R. Bartsch, in *Ullmann's Encyclopedia of Industrial Chemistry*, Wiley-VCH, 2000
3. J. Perez-Ramirez, C. Mondelli, T. Schmidt, O. F. K. Schlueter, A. Wolf, L. Mleczko, T. Dreier, Energy Environ. Sci. **4** (2011) 4786
4. T. Vidakovic-Koch, I. Gonzalez Martinez, R. Kuwertz, U. Kunz, T. Turek, K. Sundmacher, *Membranes* **2** (2012) 510
5. R. Kuwertz, I. Gonzalez Martinez, T. Vidakovic-Koch, K. Sundmacher, T. Turek, U. Kunz, *Electrochem. Commun*. **34** (2013) 320
6. I. Gonzalez Martinez, T. Vidaković-Koch, R. Kuwertz, U. Kunz, T. Turek, K. Sundmacher, *Electrochim. Acta* (2013), submitted
7. D. J. Eames, J. Newman, *J. Electrochem. Soc*. **142** (1995) 3619
8. K. Sundmacher, *J. Appl. Electrochem*. **29** (1999) 919
9. T. Vidakovic, M. Christov, K. Sundmacher, *Electrochim. Acta* **49** (2004) 2179
10. T. Vidakovic, M. Christov, K. Sundmacher, *J. Electroanal. Chem*. **580** (2005) 105
11. R. S. Yeo, J. McBreen, A. C. C. Tseung, S. Srinivasan, J. McElroy, *J. Appl. Electrochem*. **10** (1980) 393
12. B. E. Conway, G. Ping, *J. Chem. Soc., Faraday Trans*. **86** (1990) 923
13. K. Sundmacher, T. Schultz, *Chem. Eng. J*. **82** (2001) 117
14. T. Vidaković-Koch, V. K. Mittal, T. Q. N. Do, M. Varničić, K. Sundmacher, *Electrochim. Acta* **110** (2013) 94
15. C. H. Hamann, W. Vielstich, *Elektrochemie*, Wiley-VCH, Weinheim, 2005.
16. M. Umeda, K. Sayama, T. Maruta, M. Inoue, *Ionics* **19** (2013) 623
17. G. Akerlof, J. W. Teare, *J. Am. Chem. Soc.* **59** (1937) 1855
18. R. Boggio, A. Carugati, G. Lodi, S. Trasatti, *J. Appl. Electrochem*. **15** (1985) 335
19. E. Gileadi, *Electrode Kinetics for Chemists*, *Chemical Engineers, and Materials Scientists*, Wiley-VCH, New York, 1993.